2009

Closed-loop force control for a semi-automatic grinding system

Lei Yu
Iowa State University

Closed-loop force control for a semi-automatic grinding system

by

Lei Yu

A thesis submitted to the graduate faculty

in partial fulfillment of the requirements for the degree of

MASTER OF SCIENCE

Major: Industrial Engineering

Program of Study Committee:

Frank E. Peters, Major Professor

Matthew C. Frank

Palaniappa A. Molian

Iowa State University

Ames, Iowa

2009

Table of Contents

ABSTRACT

Automation of grinding of metalcastings is desirable for many reasons. The major reasons are dangerous working conditions, low productivity, and inconsistency in human operations. As an approach to the automating grinding process, a gantry-driven grinding machine is proposed to manipulate an industrial hand grinder and control the grinding force applied to the work piece. To increase the material removal rate of the grinding machine, a grinding force control method is brought forward. This method suggests that the normal grinding force should be controlled to a desired constant value. A double closed-loop grinding force control system is designed to perform the grinding force control.

This thesis develops the models of the servo system and the grinding process. Based on these models, a force controller is designed with the ability of tracking the desired force set point. The proposed closed-loop grinding force control system is verified by simulation.

Chapter 1 Introduction

1.1 General Introduction

This thesis will focus on the grinding of metalcastings. Most metalcastings require some grinding after they are shaken out of the molds. This grinding is used to remove the riser and gating contacts, possibly smooth the parting line, and correct any other surface anomalies such as burnt on sand. In this type of grinding process, the material removal is done via tedious, time-consuming manual operations such as hand grinding. Manual operations can take advantage of a skilled operator with experience and be very flexible. However, humans can also be inconsistent and less efficient. To increase the consistency and efficiency of grinding process and improve the quality of grinding surface, a three-axis gantry driven grinder with closed-loop grinding force control is proposed. This thesis addresses the problem of using a gantry to manipulate an industrial hand grinder to control the normal grinding force applied to a work piece.

The following sections introduce the structure of the gantry grinding machine, the relationship between grinding force and material removal rate, control theory related concepts, and the software MATLAB.

1.2 Proposed Grinding System

Figure 1-1 [2] shows the structure of the proposed automatic grinding system. The operator uses a joystick to control the gantry to move in X and Y directions (perpendicular to vertical grinding force). The operator also sets the grinding force according to the material, grinder wheel material, grinder rotary speed, etc. The control algorithm combines the commands from the operator and the feedback from the sensors

to decide the movement of the grinder in Z direction (vertical) to apply constant normal grinding force to the work piece, and perform appropriate grinding.

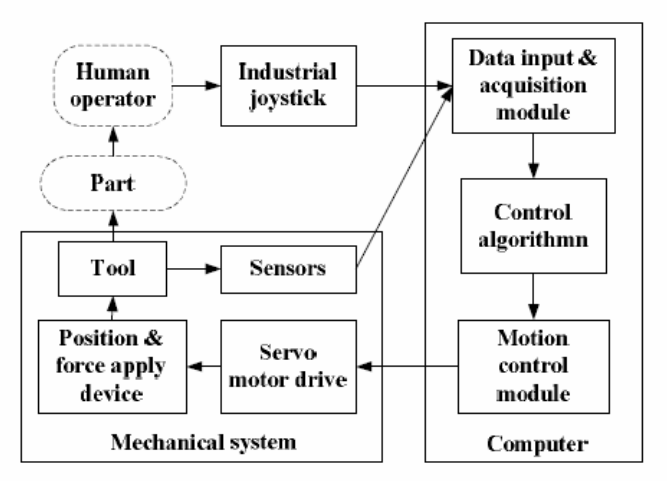

Figure 1-1 Structure of the Semi-Automatic Grinding System

The mechanical system is comprised of a three-axis gantry system, which corresponds to three degrees of freedom in the x, y, and z axes. The prototype of the gantry system is showed in Fig 1-2. The movements of the system are driven by servo motors. The force application device is attached to the gantry system. The mechanical part of the system is a gantry system driven by three servo motors.

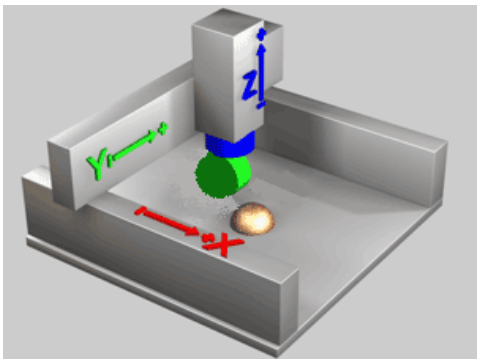

Figure1-2 Prototype of the Gantry System

A spring and damper system is used to apply the vertical force. Figure 1-3 [2] shows the structure of the force application device (head of grinder). This device is mounted on the gantry system with movement on the X and Y axes.

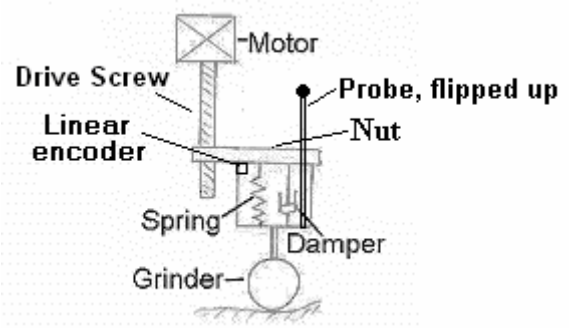

Figure 1-3 Force Application Devices

In the design, the compression spring can be controlled to generate the desired force on the part surface. The other components are a damper to reduce vibration of the system, and a linear encoder to measure the deflection of the spring that can be used to calculate the actual force applied. The spring is compressed in a housing initially. With the constraint of the housing the spring can only be compressed more. This device can only provide vertical force, so the anomalies should be positioned generally facing up to obtain better material removal results.

1.3 Grinding Force and MRR

1.3.1 Relationship between normal grinding force and material removal rate (MRR)

Several grinding force models have been proposed and recent related models were summarized by Tönshoff [9]. In some of these models material removal rate is related to normal grinding force. Hahn and Lindsay suggested that a linear relationship exists between the material removal rate and the normal force intensity [10].

$$Z_w = \Lambda_w (F_n - F_{no}) \tag{1-1}$$

Where:

Z_w - Material removal rate per unit width

Λ_w - A constant of proportionality

F_n - Normal grinding force per unit width

F_{no} - Threshold normal grinding force

Recently Ludwick et al. [11], and Jenkins and Kurfess [12] suggested the model

$$Q = K_p(F_N - F_{TH})V \tag{1-2}$$

Where Q is material removal rate, F_N is normal force, F_{TH} is the threshold value of F_N, V is the relative speed and K_p is a proportion constant.

These models suggest a linear relationship between normal grinding force and material removal rate. This linear relationship implies that a higher normal grinding force (Fn) being applied during the grinding process leads to a higher MRR which can improve the efficiency of the grinding machine. But normal grinding force Fn is limited by some conditions. For example, to prevent damage of the grinding wheel, the grinding force needs to be controlled below a critical value.

1.3.2 Increasing MRR by control of the grinding force

The objective in coarse grinding (compare to surface grinding) is rapid material removal with the desired work-piece size and shape. The performance of coarse grinding depends mainly on the material removal rate (MRR). Grinding force is a crucial issue in coarse grinding. A large depth of cut will cause a high grinding force. This can lead to many problems, such as grinding chatter, burn and exploding grinding wheels. In a coarse grinding process, the variance of normal grinding force is apparent due to the unevenness

of the part surface or unroundness of the grinder wheel. To prevent from burning the work piece or damaging the grinder, only a smaller average Fn can be applied on the part surface. Figure 1-4 shows the hypothetical grinding force variance with and without force control. The upper limit of the grinding force is to avoid the burning of work piece and damaging of the grinder. If the grinding force is controlled to a constant value, hypothetically the magnitude of variance of normal grinding force Fn will be smaller than without grinding force control. So a bigger average Fn can be applied during the grinding process. Since MRR has a linear relationship with Fn, a bigger Fn leads to a higher MRR. Therefore grinding force control could increase MRR compared to the case without grinding force control.

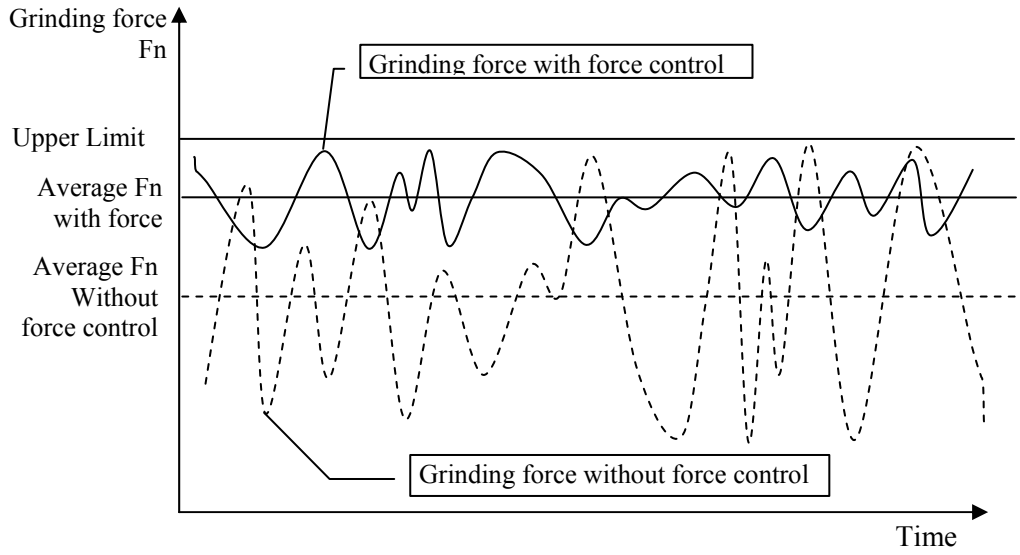

Figure 1-4 Grinding Force With and without Force Control

1.4 Related Concepts

In this thesis, the development of the models and design of the controllers are based on several important concepts and conclusions related to control theories [13]. For example, transfer function, root locus etc. This section presents those concepts and conclusions related to this thesis.

Transfer Function

A transfer function is a mathematical representation of the relation between the input and output of a LTI (linear time-invariant) system.

For example, a system has input signal x(t) and output signal y(t), the transfer function of this system is the linear mapping of the Laplace transform of the input X(s), to the output Y(s):

$$Y(s) = T(s)X(s) \tag{1-3}$$

or

$$T(s) = \frac{Y(s)}{X(s)} \tag{1-4}$$

where T(s) is the transfer function of this system.

Laplace Transform

The Laplace transform is a useful mathematical tool which can significantly reduce the effort required to solve and analyze linear differential equation models. A major benefit is that it converts ordinary differential equations to algebraic equations, which can simplify the manipulations required to obtain a solution or perform an analysis. The Laplace transform of a function $f(t)$ is defined as

$$F(s) = \ell[f(t)] = \int_0^\infty f(t)e^{-st}dt \qquad (1\text{-}5)$$

where $F(s)$ is the symbol for the Laplace transform, s is a complex independent variable, $f(t)$ is the function of time to be transformed. The inverse Laplace transform $f(t) = \ell^{-1}[F(s)]$ operates on the function $F(s)$ and converts it to $f(t)$.

The s-plane is a mathematical domain where processes are viewed as equations in the frequency domain instead of in the time domain.

Closed-loop control system

Systems that utilize feedback signal are called closed-loop control systems; an open-loop control system doesn't use feedback.

Zero, Pole and System Stability

If the transfer function of a system can be expressed as $T(s) = P(s)/Q(s)$, P(s) is the denominator of $T(s)$ and Q(s) is the numerator of $T(s)$, solutions of the equation $Q(s) = 0$ are called the poles of $T(s)$. Solutions of the equation $P(s) = 0$ are called the zeros of $T(s)$.

In control theory stability often means that for any bounded input over any amount of time, the output will also be bounded. If a system is stable, the output cannot become infinite if the input remains finite. According to the control theory, a system is stable if all of its poles locate in the left-hand side of the s-plane. An inexact explanation of this conclusion is given as below: assuming the out put of a system is given by

$$y(t) = Ae^{\alpha t} + Be^{\beta t} + \cdots \qquad (1\text{-}6)$$

where coefficients A, B, ... depend on the parameters of the system, exponents α, β, ... depend on the poles of the system. If one of the exponents has a positive real part , then part of the

solution of y(t) will increase without bound as t increases and the system is seen to be unstable (since $e^{\alpha t} \to \infty$ as $t \to \infty$ if the real part of α is positive).

For example, a system has a transfer function

$$T(s) = \frac{10}{(s-1)(s+10)} \tag{1-7}$$

System has a pole located in right hand side of the s plane (s =1). The Laplace transform of unit step response of the system is

$$Y(s) = T(s)X(s) = \frac{10}{(s-1)(s+10)}\frac{1}{s} = \frac{1}{s} - \frac{\frac{10}{11}}{s-1} - \frac{\frac{1}{11}}{s+10} \tag{1-8}$$

taking the inverse Laplace transform, the unit step response of the system is

$$y(t) = 1 - \frac{10}{11}e^{t} - \frac{1}{11}e^{-10t} \tag{1-9}$$

as $t \to \infty$, $e^{t} \to \infty$, $y(t) \to \infty$, so system is unstable.

Root Locus

The root locus is the path of the roots of the characteristic equation traced out in the s-plane while a system parameter (typically a gain) is varied. The characteristic equation is defined as the denominator of the transfer function. The root locus is a tool for analyzing single input single output (SISO) systems.

For example, a system is defined by the transfer function G(s) as in Fig 1-5. The system is controlled using a proportional controller in which the input to the system to be controlled is proportional to the difference between the input, R(s), and the output, C(s).

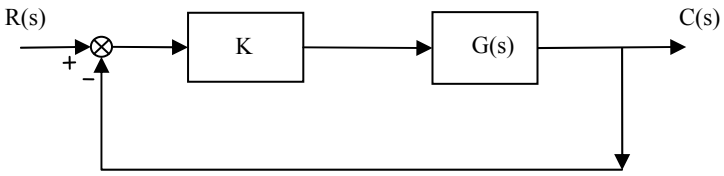

Figure 1-5 Block Diagram of an Example Control System

The closed loop transfer function of the system shown is

$$T(s) = \frac{C(s)}{T(s)} = \frac{KG(s)}{1 + KG(s)} \tag{1-10}$$

The characteristic equation is defined as

$$1 + KG(s) = 0 \tag{1-11}$$

Root locus of the closed loop system is the path of solutions of equation (1-11) as K changes from 0 to ∞.

Bode Plot

A Bode plot describes the gain and phase of a system as a function of frequency. It is a combination of a Bode magnitude plot and Bode phase plot. A Bode magnitude plot is a graph of log magnitude versus frequency to show the frequency response of a LTI (linear time-invariant) system. A Bode phase plot is a graph of phase versus frequency, also plotted on a log-frequency axis, to evaluate how much a frequency will be phase-shifted between output and input.

For example, the open loop transfer function of a system is given by G(s). The frequency response of the system is given by $G(j\omega)$. $G(j\omega)$ can also be written as

$$G(j\omega) = A(\omega)e^{j\phi(\omega)} \tag{1-12}$$

Bode magnitude plot can be drawn from $A(\omega)$ as $\omega = 0 \to \infty$ (Normally the magnitude axis is expressed as decibels: $20 \cdot \log_{10} A(\omega)$); Bode phase plot can be drawn from $\phi(\omega)$ as $\omega = 0 \to \infty$. Magnitude crossover frequency ω_c is defined as the frequency at which the open loop transfer function has unity magnitude ($20 \cdot \log_{10} A(\omega_c) = 0$). These plots show the stability of the closed-loop system through the following conclusions.

If open loop system's $\phi(\omega_c) > -180°$, then closed-loop system is stable.

The distance of the phase $\phi(\omega_c)$ above $-180°$ is called the phase margin. It is a measure of stability.

Step Response

The step response of a system is the output of the system produced by a unit step input. It is a common analysis tool used to determine system performance. The step response can be described by the following quantities.

* overshoot
* rise time
* settling time

The overshoot is the maximum swing above final value. Overshoot represents a distortion of the signal. The settling time is the time for departures from final value to sink below some specified level, say 10% of final value. Rise time is the time required for the output to change from a specified low value to a specified high value, say 90% of the final value.

Matlab and Simulink

In this thesis, the proposed closed-loop grinding force controller is designed by using Matlab and verified by Simulink. A brief description of Matlab and Simulink is given as bellow.

Matlab is a language for technical computing. It integrates computation, visualization, and programming in an easy-to-use environment where problems and solutions are expressed in common mathematical notation. Simulink, integrated with Matlab, is a software package for modeling, simulating, and analyzing dynamic systems. It provides a graphical environment that let one design, simulate, implement, and test dynamic systems.

1.5 Overview of the Force Control System

Fig 1-6 shows an overview of the force control system. There are two closed loops in this system. The inner loop is the servo system, which tracks the position command from the Force Controller. The outer loop performs the constant grinding force control which compares the force set point and force feedback signal and calculates the z position for the inner loop.

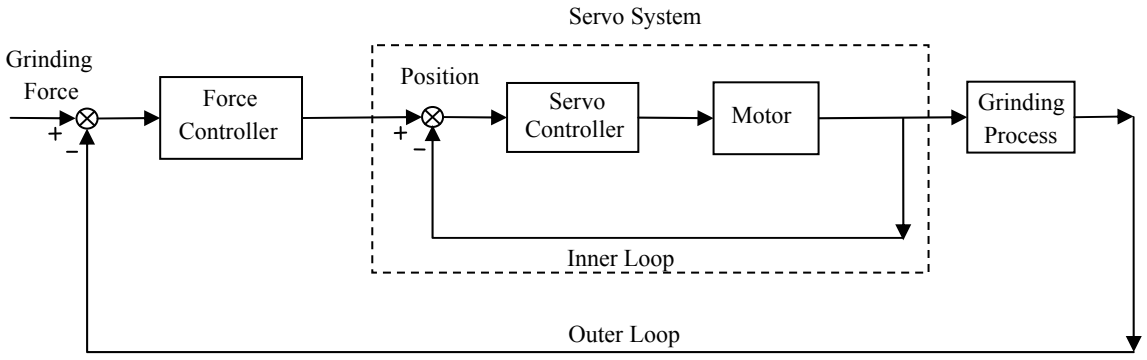

Figure 1-6 Overview of Force Control System

The remainder of this thesis is organized as follows:

- Chapter 2 derives the model of servo system and design of servo controller;
- Chapter 3 derives the model of grinding process;
- Chapter 4 presents the design of grinding force controller and simulation of force control system;
- Chapter 5 draws conclusions and discusses future work.

Chapter 2 Derivation of the Model for the Servo System and Design of the Servo Controller

This chapter derives the model of servo system and presents the design of the servo controller. The servo system (position control) is the inner loop of the force control system. Outside of it is the outer loop which controls the grinding force to be a desired constant value.

2.1 Derivation of the Model for the Servo System

In Fig 1-3, a ball screw actuator consists of several force application devices. The head of grinder (those parts mounted on the nut) can be moved along Z axis (in vertical direction). To control the grinding force, the head of grinder needs to be moved up and down according to the measure of the grinding force. A servo system is utilized to control this motion of the head of grinder.

A servo system consists of controllers, drives, motors and feedback devices. Here is a graphical representation of a typical servo system:

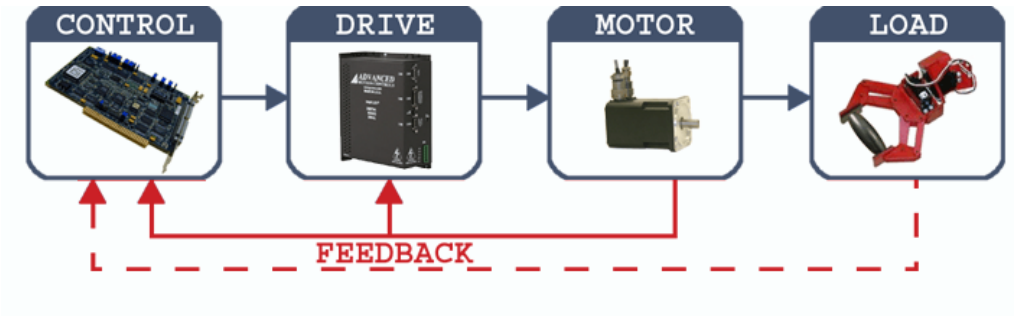

Figure 2-1 Pictorial Diagram of a Typical Servo System

The controller analyzes the errors of feedback signal and set point signal and sends a command signal to the amplifier to correct for errors. The servo drive (amplifier)

receives the command signal from a controller, amplifies the signal, and transmits electric current to a servo motor. The motor converts the current that comes from the servo drive into mechanical motion. Feedback devices are used to measure the position or velocity of the motor or load.

The proposed servo system consists of a motor, drive (ZOH, DAC, and Amp- described below), encoder and the PID controller. The elements are shown in Fig 2-2. This section presents the derivation of transfer functions of each element.

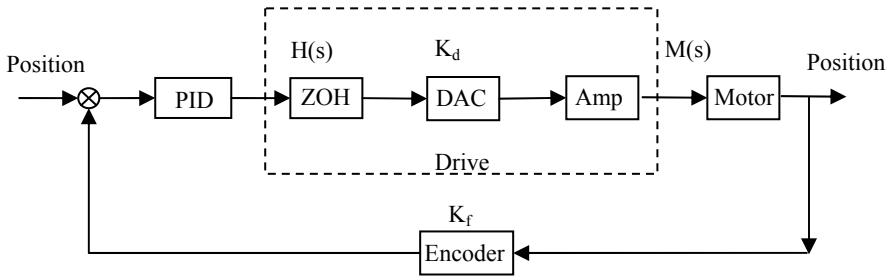

Figure 2-2 Block Diagram of a Servo System

Amplifier and Motor

The motor amplifier is configured in current drive mode. It generates a current I, which is proportional to the input voltage. It is a current source with a gain of K_a [Amp/Volt]. The transfer function relating the input voltage V to the motor position P is

$$M(s) = \frac{P}{V} = \frac{K_a K_t}{Js^2} \text{ [rad/V]} \qquad (2\text{-}1)$$

Where K_t and J are the motor and system parameters

K_a Current amplifier gain [Amp/Volt]

K_t Torque constant [N·m/Amp]

J System moment of inertia [kg·m²]

For this system, the parameters are selected as below.

$K_a = 2$

$K_t = 0.1$

$J = 2 \times 10^{-4}$

The transfer function of amplifier and motor becomes:

$$M(s) = \frac{P}{V} = \frac{1000}{s^2} \tag{2-2}$$

Encoder

The encoder generates N pulses per revolution. It outputs two signals, Channel A and B, Which are in quadrature. The model of the encoder can be represented by a gain of

$$K_f = \frac{4N}{2\pi} \text{[count/rad]} \tag{2-3}$$

where

N Encoder line density [count/rad]

If the line density of encoder is 1000 [count/rev], the transfer function of encoder is

$$K_f = \frac{4 \times 1000}{2\pi} = 637 \tag{2-4}$$

DAC

The DAC converter converts a digital number to an analog voltage. The input range of the numbers is 65536 and the output voltage is +/- 10V or 20V. Therefore, the effective gain of the DAC is

$$K_d = \frac{20}{65536} = 0.0003\,[\text{Volt/count}] \tag{2-5}$$

ZOH

The ZOH, or zero-order-hold, represents the effect of the sampling process, where the motor command is updated once per sampling period. The effect of the ZOH can be modeled by the transfer function

$$H(s) = \frac{1}{\frac{T}{2}s + 1} \tag{2-6}$$

where

T --- sampling period [s]

For this system, sampling period is 1ms, so the transfer function of ZOH becomes:

$$H(s) = \frac{2000}{s + 2000} \tag{2-7}$$

Plant Transfer Function

The combination of all the elements above is the plant (the combination of process and actuator.) transfer function, $L(s)$ which is

$$L(s) = M(s)K_f K_d H(s)$$

$$= \frac{1000}{s^2} \bullet 637 \bullet 0.0003 \bullet \frac{2000}{s + 2000} \tag{2-8}$$

$$= \frac{3.822 \bullet 10^5}{s^2(s + 2000)}$$

2.2 Design of the Servo Controller

To achieve the position control, a servo controller (PID controller) is added in series. A proportional–integral–derivative controller (PID controller) is a feedback control mechanism which is commonly used in industrial control systems. A PID controller corrects the error between a process feedback and a desired setpoint by calculating a corrective output that can adjust the process accordingly. The PID controller calculation includes three separate parameters; the Proportional, the Integral and the Derivative values. The Proportional value determines the reaction to the current error which can reduce the rise time and steady-state error, the Integral value will have effects of removing steady-state error, and the Derivative value will increase the stability of a system. The weighted sum of these three correction values is used to adjust the process.

The closed loop system is showed in Fig 2-3. The open loop transfer function $G_o(s)$ becomes

$$G_o(s) = G_{PID}(s)L(s) \tag{2-9}$$

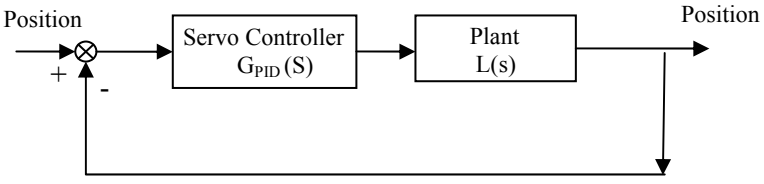

Figure 2-3 Servo System

Fig 2-4 presents the root locus of the system without a controller.

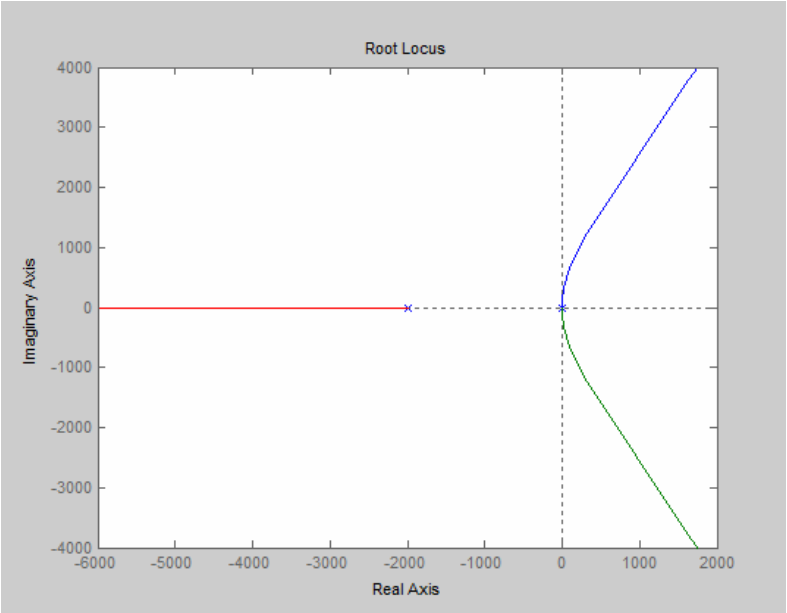

Figure 2-4 Root Locus of Plant

Parts of the root loci extend to the right hand side s-plane, so this system is not stable. Adding a PID controller to the system, the path of the root loci can be shifted which leads to the change of the performance of the system. To stabilize the system and obtain a closed-loop step response with small overshoot and fast rise time, a PID controller is added in series.

The Bode plot of plant L(s) is showed in Fig 2-5. From the plot, some important data can be read. The magnitude of L(s) at the frequency ω_c = 500 is -62.6 dB and the phase of L(s) at the frequency ω_c = 500 is -194 deg.

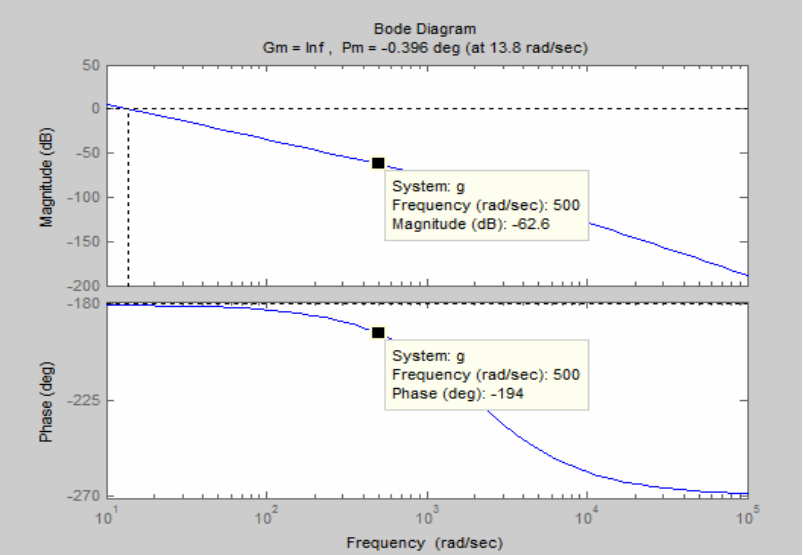

Figure 2-5 Bode Plot of Plant

The parameters of the objective controller affects the performance of servo system, they also affects the performance of the whole force control system. As a start point they are selected by experiential data. They might need to be modified depending on the simulation of the whole system. This process repeats until the performance of both servo system and the whole force control system meet the requirements. This thesis only presents the determined parameters. The servo controller $G_{PID}(s)$ is selected so that $G_o(s)$ has a crossover frequency (the frequency at which the magnitude of the open loop transfer function is unity) of 500 rad/s and a phase margin (a measure of stability of a feedback system, it is the phase difference between the phase of open loop transfer function at crossover frequency and -180°) 70 degrees.

This requires that

$$\left|G_o(j500)\right| = 1$$
$$\arg\left[G_o(j500)\right] = -110^\circ \qquad (2\text{-}10)$$

So $G_{PID}(s)$ must have magnitude of

$$\left|G_{PID}(j500)\right| = \left|\frac{G_o(j500)}{L(j500)}\right| = \frac{1}{0.0007416} = 1349 \tag{2-11}$$

and a phase

$$\begin{aligned} \arg[G_{PID}] &= \arg[G_o(j500)] - \arg[L(j500)] \\ &= -110° + 194° = 84° \end{aligned} \tag{2-12}$$

A PD controller is used to provide the correction.

$$G_{PID}(s) = P + sD \tag{2-13}$$

so

$$\begin{aligned} \left|G_{PID}(j500)\right| &= P + j500D = 1349 \\ \arg[G_{PID}(j500)] &= \tan^{-1}(\frac{500D}{P}) = 84° \end{aligned} \tag{2-14}$$

The solution of these equations leads to

$$P = 1349\cos 84° = 141 \tag{2-15}$$

$$D = \frac{1349\sin 84°}{500} = 2.68 \tag{2-16}$$

$$G_{PID}(s) = P + sD = 141 + 2.68s \tag{2-17}$$

$$G_o = L(s)G_{PID}(s) = \frac{3.822 \bullet 10^5 (141 + 2.68s)}{s^2(s + 2000)} \tag{2-18}$$

This PD controller equivalent to add a zero to the open system and the zero is $s = -141/2.68 = -52.6$. The step response of closed-loop system is showed in Fig 2-6

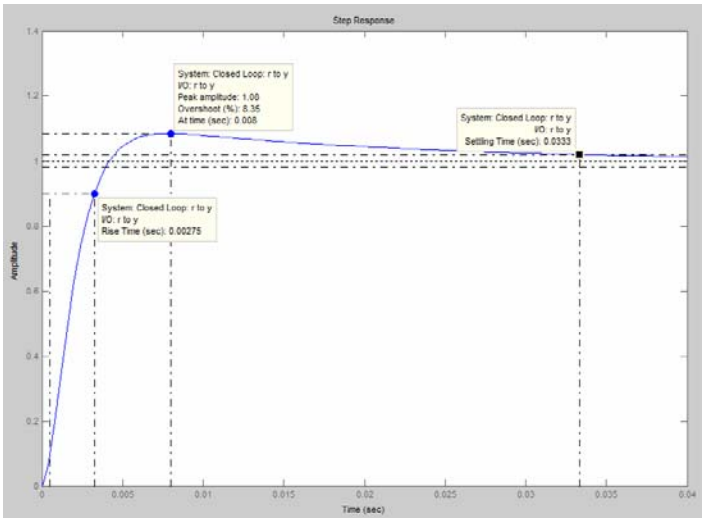

Figure 2-6 Closed Loop System Step Response with PD Controller 1

From Fig 2-5, 90% rise time is read as 0.00275 second, overshoot is 8.35%, and settling time is 0.0333 second. These parameters are used as basic data to tune system. These data would satisfy the requirement of the servo system and help the outer loop to obtain a desired response. Open and closed-loop transfer functions of the servo system are as below:

$$G_o = L(s)G_{PID}(s) = \frac{3.822 \cdot 10^5 (141 + 2.68s)}{s^2(s + 2000)} \tag{2-19}$$

$$G_{servo}(s) = \frac{G_o}{1 + G_o} = \frac{1.024 \cdot 10^6 s + 5.389 \cdot 10^7}{s^3 + 2000s^2 + 1.024 \cdot 10^6 s + 5.389 \cdot 10^7} \tag{2-20}$$

The open loop system root locus with PD controller is presented in Fig 2-7. With the correction of the PD compensator, now all loci locate in left hand s-plane which means the closed loop system is stable.

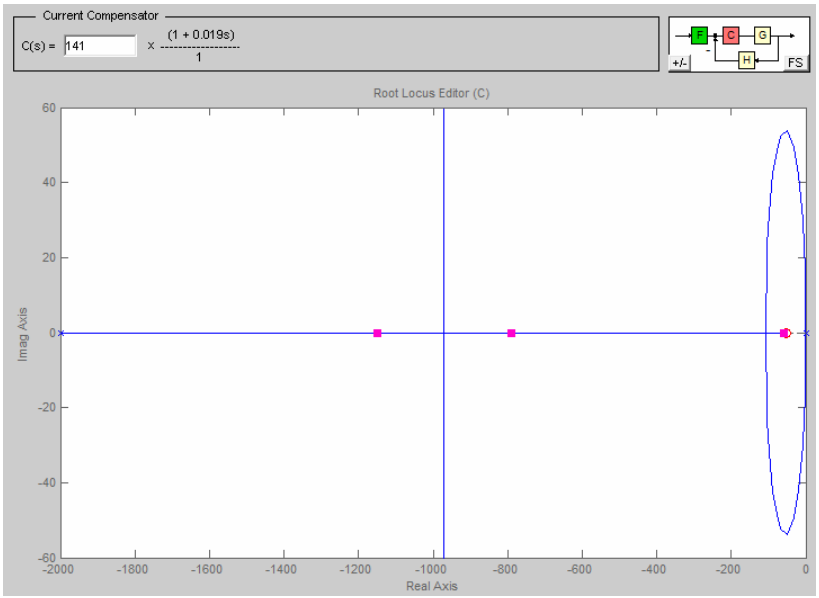

Figure 2-7 Root Locus of Open Loop System with PD Controller 2

The open loop system with PD controller is a second order system, so for step and ramp input, there is no steady state error in the output.

Chapter 3 Derivation of the model of Grinding Process

3.1 Grinding Force Equation

In designing grinding system, grinding force models are necessary to build up the dynamic model of the system. Werner analyzed the relationships of grinding force and other parameters related to the grinding process and suggested the following equation [5]. For surface grinding, the normal component of the total grinding force per unit of grinding width is given by:

$$F_n' = K\left[C_1\right]^{\gamma}\left[\frac{v_w}{v_s}\right]^{2\varepsilon-1}\left[a\right]^{\varepsilon}\left[D\right]^{1-\varepsilon}$$

$$\text{with} \qquad (3\text{-}1)$$

$$\varepsilon = \frac{1}{2}\left[(1+n)+\alpha(1-n)\right]$$

$$\gamma = \beta(1-n)$$

where

F_n'	normal grinding force per unit of grinding width
K	proportionality factor
C_1	cutting edge density
γ	exponential parameter of grinding force equation
v_w	work speed
v_s	wheel speed
ε	exponential parameter of grinding force equation
a	depth of cut
D	equivalent wheel diameter
n	exponent describing cutting force versus chip cross section
α	exponential coefficient
β	exponential coefficient

The value of the exponential parameter of grinding force equation ε is in the range of

$0.5 \le \varepsilon \le 1$. Equation (3-1) describes the grinding force as a function of all relevant parameters.

To derive the model of grinding process for the controller design, only depth of cut a is considered as a variable, equation (3-1) can be simplified as

$$F_n^{'} = K_F a^{\varepsilon} \tag{3-2}$$

where

K_F Proportionality factor

In this model, the surface of the work piece will be considered as roughly horizontal, so the normal grinding force is in vertical direction. Equation (3-2) suggests a none-linear relationship between normal grinding force and depth of cut. To simplify the model to a linear relationship, the ratio of the normal grinding force to depth of cut is assumed to be a constant value K_2 [1].

$$F_n = K_2 a \tag{3-3}$$

So the grinding process could be modeled as a spring with a spring constant K_2

3.2 Model of Grinding Process

For the feed speed in X and Y directions, with the encoder feedback signal the motion control circuit will be configured as a position and speed closed-loop controller. This is a classic application for the motion control card and this thesis will not cover the application of the feed control.

For the grinding force, while the surface of anomaly changes or the surface of the part changes, the grinding force is controlled to keep a constant value by adjusting the Z position of the head of grinder (the parts mounted on the nut of the grinding force application device showed in Figure 1-3). A model of grinding process is needed for the

design of the controller. This model describes the dynamic relationship between the Z position and the grinding force.

In Fig 3-1 symbols are defined as following:

K_1 --- spring constant

K_2 --- equivalent spring constant of grinding process

m --- mass of grinder head

b --- damping constant

z(t) --- vertical direction displacement of gantry

p(t) --- vertical direction displacement of grinding wheel

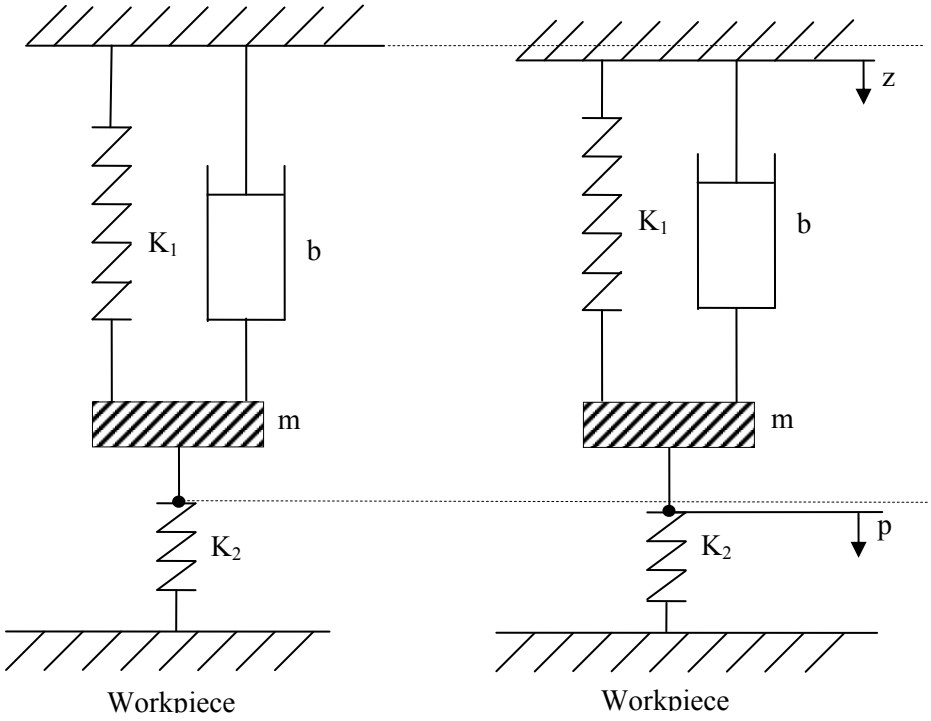

3-1 a Initial position of head of grinder

3-1 b After head of grinder moves a displacement in Z direction

Figure 3-1 Modeling of the Grinding Process

The displacements z, p are measured from a static equilibrium position. Assuming the deformations of spring 1 and spring 2 are x_1 and x_2 respectively.

$$K_1 x_1 + mg = K_2 x_2 \tag{3-4}$$

Assuming the gantry moves a displacement z in vertical direction, and the grinding wheel moves a displacement p in the vertical direction. The dynamic function of the grinder is given by:

$$K_1(x_1 + z - p) + mg - K_2(x_2 + p) + b(\dot{z} - \dot{p}) = m\ddot{p} \tag{3-5}$$

Because z and p are defined in a static equilibrium position, the constants can be canceled by substituting $K_1 x_1 + mg$ for $K_2 x_2$.

The equation (3-5) converts to

$$K_1(z - p) - K_2 p + b(\dot{z} - \dot{p}) = m\ddot{p} \tag{3-6}$$

Incremental grinding force f can be calculated as

$$f = K_2 p \tag{3-7}$$

substitute $p = \frac{f}{K_2}$ into (3-6)

$$K_1(z - \frac{f}{K_2}) - f + b(\dot{z} - \frac{\dot{f}}{K_2}) = m\frac{\ddot{f}}{K_2} \tag{3-8}$$

$$b\dot{z} + K_1 z = \frac{1}{K_2}(m\ddot{f} + b\dot{f} + K_1 f + K_2 f) \tag{3-9}$$

take the Laplace transform of both sides of equation (3-9)

$$(bs + K_1)Z(s) = \frac{1}{K_2}(ms^2 + bs + K_1 + K_2)F(s) \tag{3-10}$$

Where

F(s) --- Laplace transform of f(t)

Z(s) --- Laplace transform of z(t)

z(t) is selected as the input signal of grinding process and f(t) is selected as output signal. The transfer function of the grinding process $G_p(s)$ is given by:

$$G_p(s) = \frac{F(s)}{Z(s)} = \frac{K_2(bs + K_1)}{ms^2 + bs + K_1 + K_2} \tag{3-11}$$

Block diagram of the grinding process is shown below in Fig 3-2.

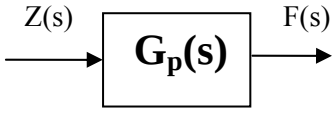

Figure 3-2 Block Diagram of Model of the Grinding Process

To simplify the design of the controller, the damper is ignored, so b=0. Here the parameters are estimated as:

$m = 15 \quad kg$

$K_1 = 9 \cdot 10^4 \quad N/m$

$K_2 = 2.22 \cdot 10^6 \quad N/m$

So the transfer function of the grinding process could be described by the following equations.

$$G_p(s) = \frac{K_2 K_1}{ms^2 + K_1 + K_2} = \frac{1.98 \cdot 10^{11}}{15s^2 + 2.29 \cdot 10^6} \tag{3-13}$$

Ball Screw

Ball screw transfers radian position of the motor shaft to z position, the transfer function, K_B [m/rad], is

$$K_B = 8 \cdot 10^{-4} \qquad \text{(about 1/5 inch per revolution)}$$

Chapter 4 Design of Controller and Simulation Results

This chapter presents the design of grinding force controller which closes the outer loop of the grinding force control system. The plant of the control system includes servo system and the grinding process.

4.1 Design of Grinding Force Controller

Figure 4-1 describes the components of the whole grinding force control system. To stable the whole system and obtain a desired performance, this section will determine the grinding force controller G_c. The transfer functions of servo system and grinding process have been determined in chapter 2 and 3. Plant (servo system and grinding process) transfer function can be derived based on these transfer functions. A design tool (SISOTOOL) is used to find the grinding force controller.

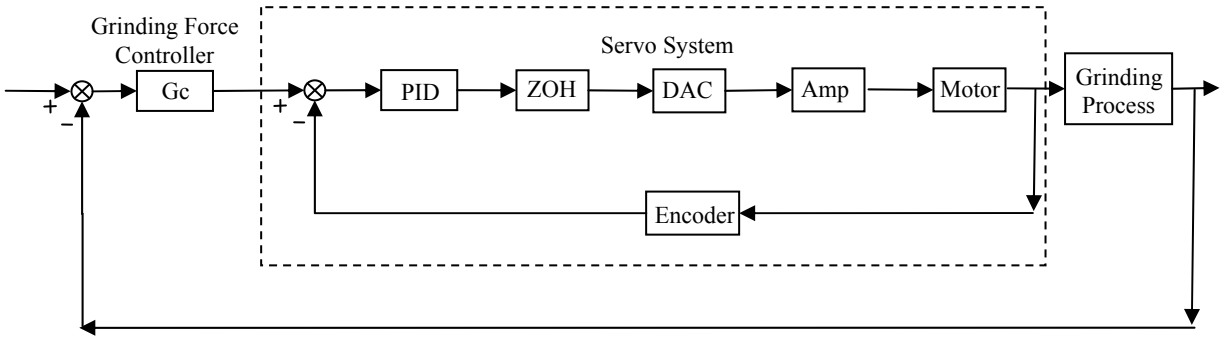

Figure 4-1 Grinding Force Control System

As presented in chapter 2 and 3, the transfer function of plant (servo system and grinding process) includes:

Servo system transfer function (same as equation (2-20)):

$$G_{servo}(s) = \frac{1.024 \cdot 10^6 s + 5.389 \cdot 10^7}{s^3 + 2000s^2 + 1.024 \cdot 10^6 s + 5.389 \cdot 10^7} \tag{4-1}$$

Grinding process transfer function (same as equation (3-11)):

$$G_p(s) = \frac{1.98 \cdot 10^{11}}{15s^2 + 2.29 \cdot 10^6} \tag{4-2}$$

So the transfer function of the plant will be:

$$G_{plant} = G_{servo}(s) G_1(s) K_B$$

$$= \frac{1.024 \cdot 10^6 s + 5.389 \cdot 10^7}{s^3 + 2000s^2 + 1.024 \cdot 10^6 s + 5.389 \cdot 10^7} \cdot \frac{1.98 \cdot 10^{11}}{15s^2 + 2.29 \cdot 10^6} \cdot 8 \cdot 10^{-4} \tag{4-3}$$

$$= \frac{1.622 \cdot 10^{14} s + 8.536 \cdot 10^{15}}{15s^5 + 30000s^4 + 1.765 \cdot 10^7 s^3 + 5.388 \cdot 10^9 s^2 + 2.346 \cdot 10^{12} s + 1.234 \cdot 10^{14}}$$

The open loop system has one real zero

$$z = -52.61$$

and three real poles

$$p_1 = -1150$$

$$p_2 = -790.5$$

$$p_3 = -59.27$$

and a pairs of complex poles

$$p_{4,5} = \pm 390.768i$$

Fig 4-2 and Fig 4-3 show the root locus and unit step response of the open loop system. As mentioned in Chapter 1, two of the loci extend to right hand side of s- plane which means the system is not stable.

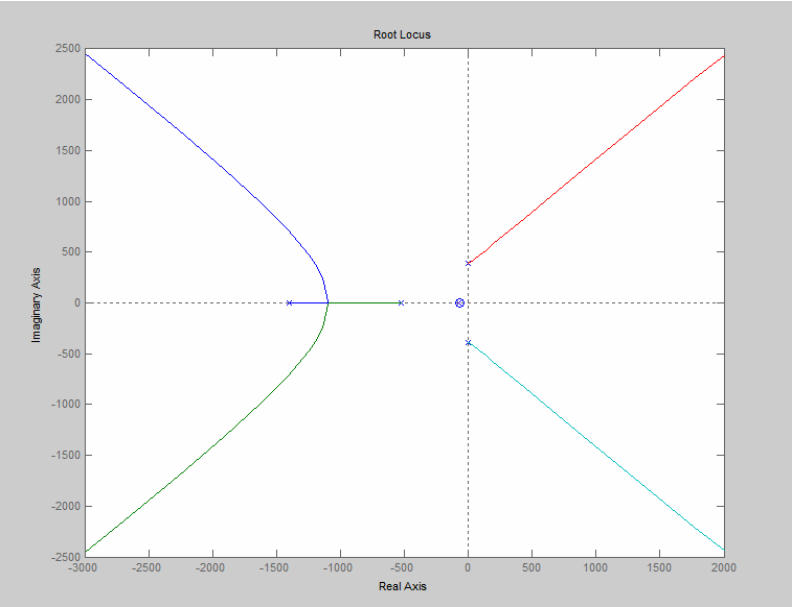

Figure 4-2 Root Locus of Plant

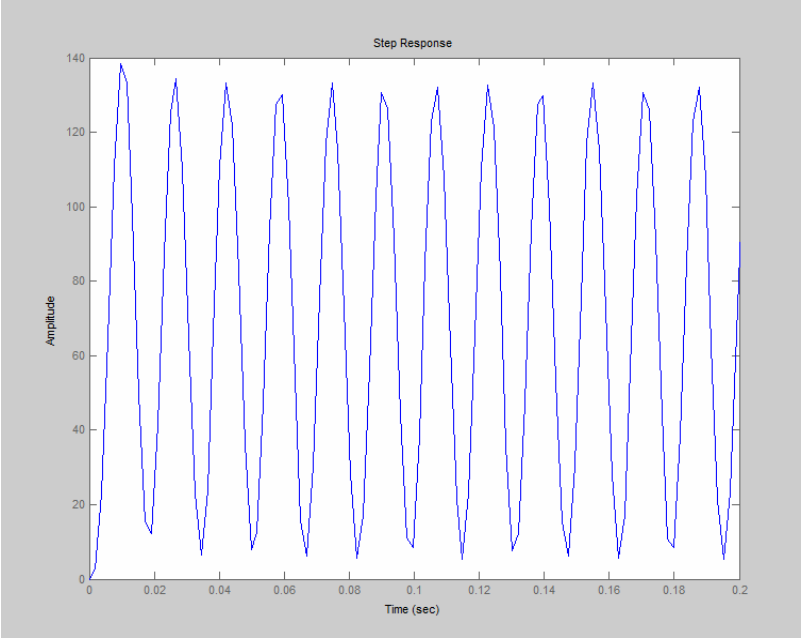

Figure 4-3 Step Response of Open Loop System without Controller

SISOTOOL (single input single output system design tool) is used to find the controller. To increase the type of system, a pure integrated unit is added. To stable the system, two complex zeroes are added.

$$s = -70 \pm 378\,j$$

And a real zero $s = -190$ is added also to stable the system.

Under the effect of the these zeros and poles, the new open loop system loci presented in Fig 4-4 now all locate in the left hand side s-plane.

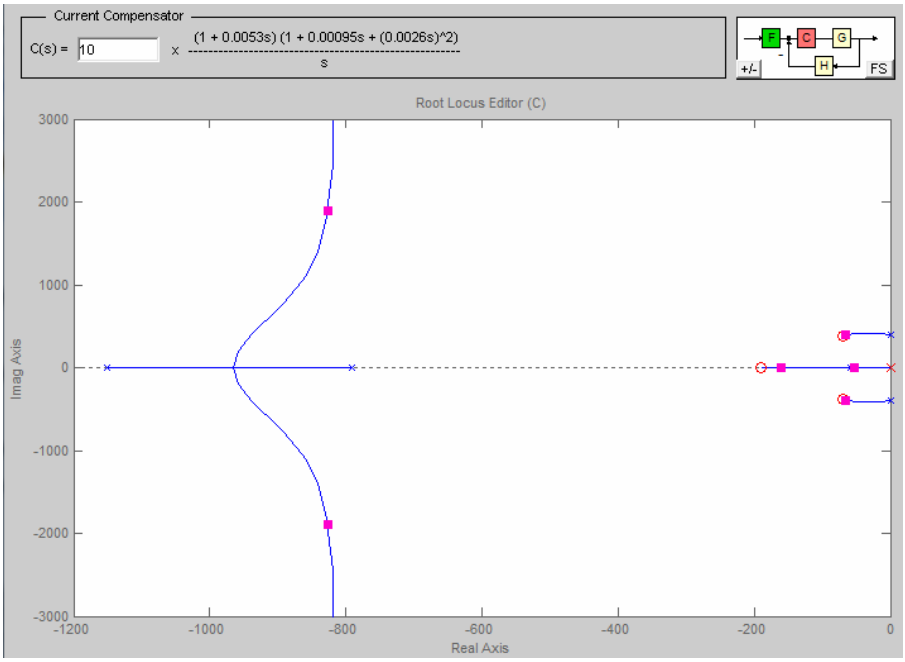

Figure 4-4 Locus Diagram of Open Loop System with Compensator

Transfer function of Compensator is as below:

$$G_c(s) = \frac{10(1+0.0053s)\left[1+0.00095s+(0.0026s)^2\right]}{s} \qquad (4\text{-}4)$$

Reading from the Bode plot of the open system with the compensator, system is a stable loop and has a phase margin of 47.6° at crossover frequency 1710 rad/sec.

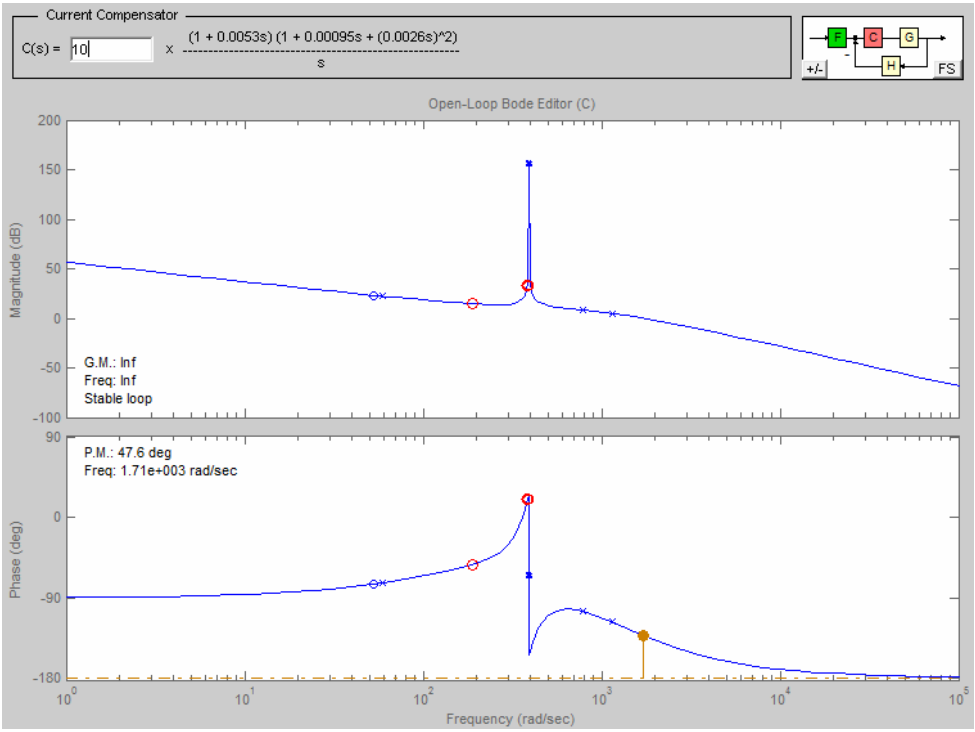

Figure 4-5 Bode Plot of Open Loop System with Compensator

Step response of the force control system with this compensator is showed in Fig 4-6

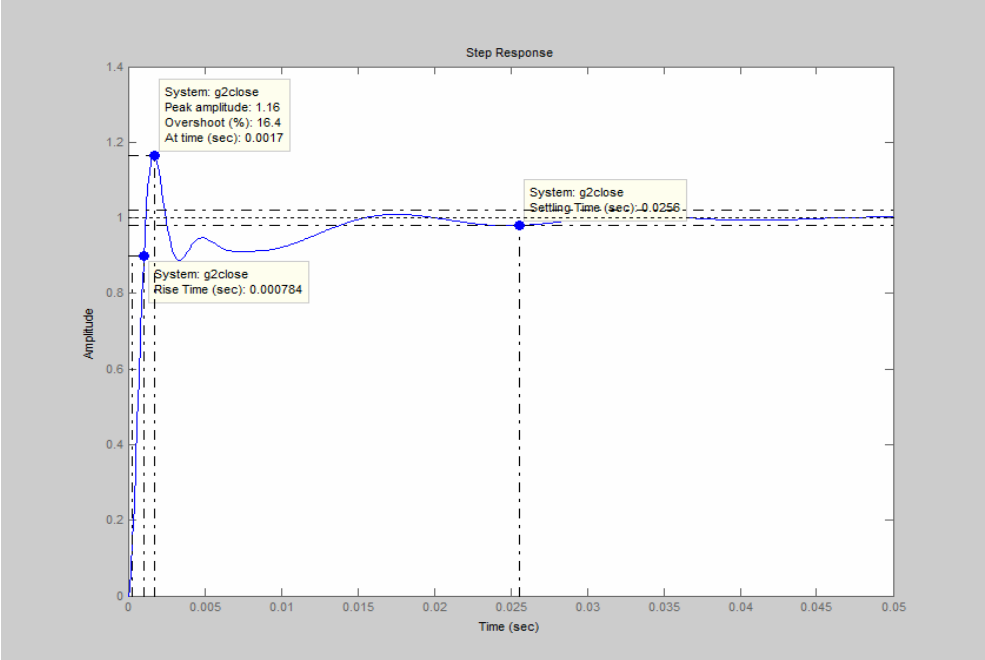

Figure 4-6 Step Response of Closed-Loop System with Compensator

From Fig 4-6, 90% rise time is read as 0.000784 second, overshoot is 16.4%, and settling time is 0.0256 second.

4.2 Simulation Results

Simulation of the grinding force control system is executed in the Simulink environment which is a build-in software package of Matlab.

Simulation block diagram is showed in Fig 4-7.

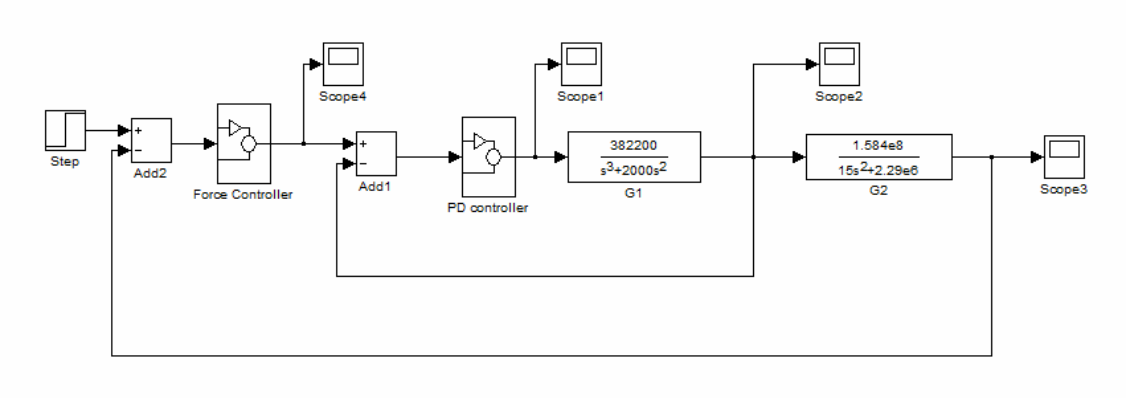

Figure 4-7 Simulation Block Diagram of Grinding Force Control System

Unit step response of the grinding force control system is showed below in Fig 4-8. This response shows that system is stable and the steady state error is zero which means the system can follow the input signal. The overshoot is about 8% and rise time is about 0.01 second. Settling time is about 0.05 second. Results show that grinding force can be controlled to a desired value.

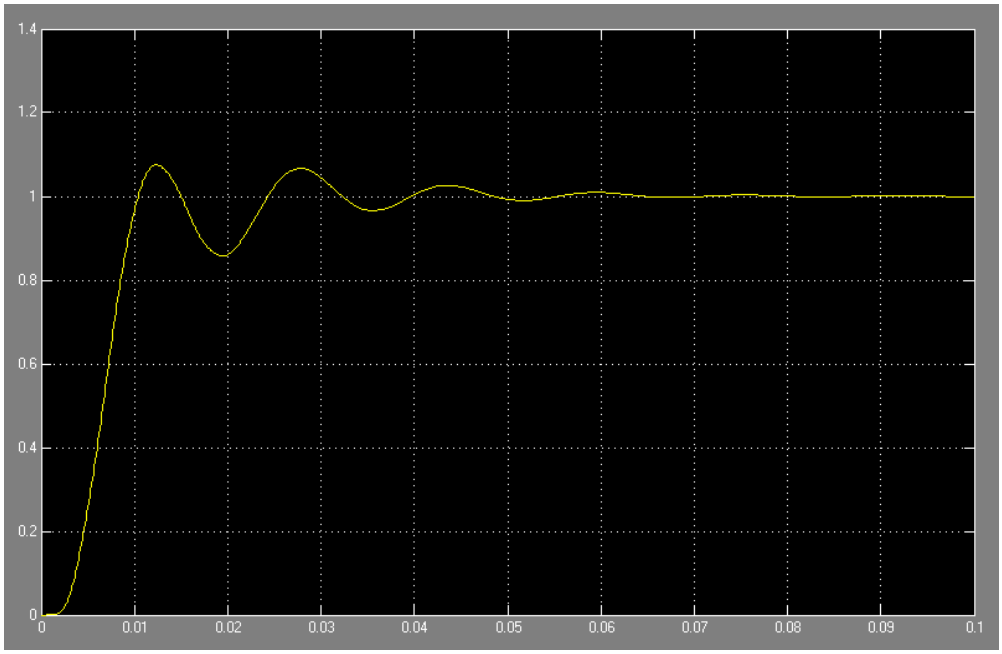

Figure 4-8 Simulation Result-Unit Step Response

Detailed simulation block diagrams of PD inner loop controller and the grinding force controller are presented in Fig 4-9 and Fig4-10 respectively.

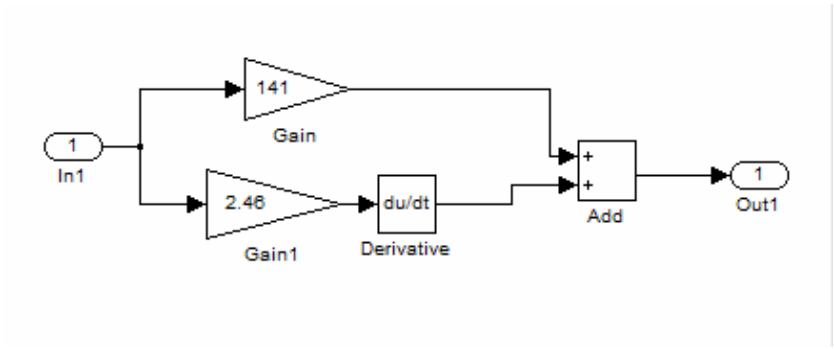

Figure 4-9 Block Diagrams of PD Controller

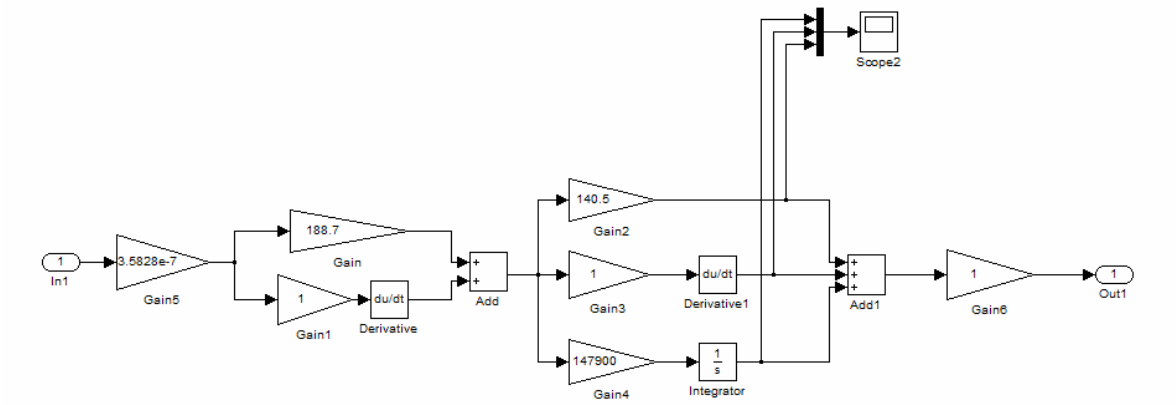

Figure 4-10 Block Diagrams of Grinding Force Controller

Chapter 5 Conclusion and Future Work

In this thesis, a three-axis gantry driven grinding system has been proposed. To increase the material removal rate, the grinding force control method is brought forward. A model of servo system is derived and a servo controller is designed. This paper also presents a model of grinding process and the design of a grinding force controller. The force control system is simulated using the commercial software Simulink package. The simulation result shows that the proposed double closed-loop force control system can follow a step force input.

Although the controller remained stable for a wide range of conditions, the robustness of the controller to disturbances and parameter variations should be determined. An analysis of feed-forward or no-linear controller could be performed to obtain a better performance. More experimentations or simulations could be performed to support the hypothesis that grinding force control increases MRR.

Reference

1. C. H. Liu, A. Chen, Y.T. Wang, C.C. A. Chen, 2004, Modelling and simulation of an automatic grinding system using a hand grinder, Int J Adv Manuf Technol (2004) 23: 874–881

2. D. Wang, 2007, A general material removal strategy based on surface sampling and reconstruction on unknown objects, PhD dissertation, Iowa State University

3. Y.T. Wang, Y.J. Jan 2001 Grinding force models in finishing processes, 2001, IEEE/ASME International Conference on Advanced Intelligent Mechatronics Proceedings ,B-12 July 2001 Como. Italy

4. Motion control – NI motion user manual, 2006 National Instruments

5. G. Werner, 1978, Influence of Work Material on Grinding Forces, CRIP, Volume 27, No. 1,1978,p. 243-248

6. C. H. Liu, A. Chen, Y.T. Wang, C.C. A. Chen, 2005, Grind force control in an automatic surface finishing system, Journal of Materials Processing Technology 170 (2005) 367-373

7. M.H.Liu, 1995, Force-controlled fuzzy-logic-based robotic deburring, Control Eng. Practice, Vol3, No. 2,pp189-201,1995

8. Y.T. Wang , Y.J.Jan, 2000 A robot assisted finishing system with an active torque controller, Proceedings of the 2000 IEEE international conference on robotics & automation, San Francisco, CA, April 2000

9. HK Tönshoff, J Peters, I Inasaki, T Paul (1992) Modeling and simulation of grinding processes. Ann CIRP 41:677-688

10. RS Hahn, RP Lindsay (1971) Principles of grinding, part 1: Basic relationships in precision grinding. Machinery, pp 55-62

11. SJ Ludwick, HE Jenkins, TR Kurfess (1994) Determination of dynamic grinding model. Trans ASME Dyn Syst Contr 55:843-849

12. HE Jekins, TR Kurfess (1996) Optimization of real-time multivariable estimation in grinding. Trans ASME Dyn Syst Contr 58:365-370

13. Benjamin C. Kuo (1994) Automatic Control Systems 7th edition, Prentice Hall

Acknowledgements

Many people contributed to the work presented in this thesis and essentially made the thesis possible at all.

First of all, I would like to thank my advisor, Dr. Frank Peters, for his inspiring way to guide me to a deeper understanding of the knowledge on material removal process. Dr. Peters provides me with great details of the material removal problem in the metalcasting grinding operation. I really appreciate the discussions with Dr. Frank which are always productive and innovative. I am also grateful to Dr. Molian. My gratitude also goes to other students and colleagues at the Department of Industrial and Manufacturing Systems Engineering for developing a good working atmosphere, especially Danni Wang, Brian Harwood, Xiaoming Luo, and Fanqi Meng, for their assistance and companionships throughout my work.

Last but not least, I am greatly grateful to my wife, my baby girl and my family for their understanding and support during the entire period of my study.